

Counting statistics of X-ray detectors at high counting rates

David Laundry* and Stephen Collins

Daresbury Laboratory, Warrington, Cheshire WA4 4AD, England. E-mail: d.laundry@dl.ac.uk

Modern synchrotron radiation sources with insertion devices and focusing optics produce high fluxes of X-rays at the sample, which leads to a requirement for photon-counting detectors to operate at high counting rates. With high counting rates there can be significant non-linearity in the response of the detector to incident X-ray flux, where this non-linearity is caused by the overlap of the electronic pulses that are produced by each X-ray. A model that describes the overlap of detector pulses is developed in this paper. This model predicts that the correction to the counting rate for pulse overlap is the same as a conventional dead-time correction. The model is also used to calculate the statistical uncertainty of a measurement and predicts that the error associated with a measurement can be increased significantly over that predicted by Poisson ($N^{-1/2}$) statistics. The error differs from that predicted by a conventional dead-time treatment.

Keywords: X-ray detectors; counting statistics; high counting rates; non-linear responses.

1. Introduction

The purpose of an X-ray detector is to measure the flux of a beam of X-rays, where the X-ray flux is commonly expressed as the number of X-ray photons in the beam in a given energy bandwidth per unit time. X-ray detectors may be classified as one of two types:

(i) integrating detectors, in which the X-rays are converted into an analogue electrical signal, the size of the signal being proportional to the X-ray power;

(ii) photon-counting detectors, in which each X-ray generates a pulse and the number of pulses counted in a fixed time period is proportional to the X-ray flux.

This paper is concerned with photon-counting detectors, such as scintillation, solid-state and gas-proportional detectors (Knoll, 1989). We assume that the flux of X-rays being measured is constant over time or that any time structure is on a much shorter time scale than the detector response. Photon-counting detectors rely on the absorption of an incident X-ray followed by some physical process that converts the energy of the absorbed X-ray into an electronic pulse. It is a feature of photon-counting detectors that the detection efficiency can approach 100%, and, in the low-count-rate regime, every X-ray absorbed in the detector generates a pulse so that there is a linear relationship between the mean number of counts in a counting period and the X-ray flux. To process and count the number of pulses, the detector is connected to electronics known as the counting chain. The counting chain may also allow the energy of each absorbed X-ray to be determined if the size of the pulse depends on the energy of the X-ray. Photon-counting detectors are used in applications where accurate measurement of X-ray flux is required, where the X-ray flux is not too high and where energy resolution is required.

At synchrotron radiation sources, photon-counting detectors are used in a variety of experiments. The best photon-counting detector for a particular application depends on the energy resolution and the

count rate that is required. In general, if higher energy resolution is required, the detector will be limited to lower count rates. A number of applications of photon-counting detectors at synchrotron sources are possible, for example

- (i) measuring the X-ray flux in a monochromatic beam,
- (ii) measuring the X-ray flux at a fundamental energy while at the same time rejecting X-rays at harmonic energies,
- (iii) selecting or removing specific fluorescence signals,
- (iv) determining the X-ray spectrum (energy dispersive measurements).

In the first application, the detector is not required to have any energy-resolving capability, although energy resolution will allow background radiation at other energies to be discriminated. Detectors in the second category are required to count X-rays with a fundamental energy but not X-rays with the harmonic energy. The harmonic energy from a monochromator may have two or three times the fundamental energy, and therefore moderate energy resolution is required of the detector. In the third category, better energy resolution is required, as the background may include the exciting radiation and other fluorescent radiation, which may be close in energy to the fluorescent radiation of interest. The fourth category also requires high energy resolution, as the detector, rather than the incident radiation, is used to provide the energy resolution of the experiment.

The stages in the counting chain are as follows:

(i) Amplification and shaping – takes the electronic pulse from the detector and applies filtering, shaping and amplification to give a sharp pulse of suitable amplitude.

(ii) Analysis – selects pulses according to the pulse height to give energy sensitivity.

(iii) Accumulation – counts the pulses in one or multiple channels in a fixed time period.

The amplification and shaping stage may be accomplished by a single linear amplifier. The gain of the amplifier may be selected so as to produce pulses of suitable amplitude for the next stage, and the shaping time of the amplifier may be increased to filter out more electronic noise (at the expense of increasing the time duration of the pulse). The analysis stage is used to measure the energy of the X-rays. The analysis stage may use a single channel that produces an output pulse only for pulses whose height is between predefined lower and upper levels, *i.e.* a single-channel analyser (SCA), or may use many channels so that each pulse is converted into an integer value in proportion to the height of the pulse, *i.e.* a multi-channel analyser (MCA). The purpose of the accumulation stage is to count the number of pulses in each channel in a fixed time period.

2. The statistics of photon counting

To measure X-ray flux, the detected X-rays are counted over a fixed time, T . When the counting rate is low, so that every X-ray is counted, the probability of there being n counts is given by a Poisson distribution,

$$P_n(\lambda) = \lambda^n e^{-\lambda} / n!, \quad (1)$$

where λ is a constant. This distribution reflects the random nature of the arrival of X-rays in the detector. The mean number counted is given by

$$\bar{n} = \sum_{n=0}^{\infty} n P_n(\lambda).$$

It is easy to show that for a Poisson distribution, (1), this reduces to $\bar{n} = \lambda$. λ is therefore the mean (or expected) number of X-rays

counted in a time T , and λ/T is the X-ray flux. The error in the number of X-rays counted is given by the standard deviation of the distribution,

$$s(n) = \overline{(n - \bar{n})^2}^{1/2} = \sum_{n=0}^{\infty} (n - \bar{n})^2 P_n(\lambda).$$

It is again easy to show that for a Poisson distribution, (1), this reduces to $s(n) = \lambda^{1/2}$. Therefore, for a measurement (labelled k) that yields n_k counts in a time interval T , the X-ray flux can be estimated as n_k/T , with an error of $n_k^{1/2}/T$. The fractional error in the measurement of the X-ray flux is therefore $n_k^{-1/2}$. For a large number of counts, n , the Poisson distribution can be approximated as a normal distribution with standard deviation $s(n)$.

The aim of an X-ray experiment is to measure some property of a sample that is exposed to an incident X-ray beam, and this measurement is achieved by examining the flux of the X-ray beam that has interacted with the sample (for example, by scattering or absorption in the sample). To perform such measurements accurately requires a small fractional error in the measurement, so that $n_k^{-1/2}$ must be small and therefore n_k must be large. n_k can be increased by making the counting period longer or by using a more intense incident beam.

3. High counting rates

It is well known that the relationship between the X-ray flux incident on the detector and the mean number of counts becomes non-linear at high counting rates (see, for example, Jenkins *et al.*, 1981; Knoll 1989), thus limiting the count rate that can be achieved by a detector. The source of this non-linearity is the inability of the detector and the counting chain to resolve X-ray pulses when the time separation between individual pulses becomes too small. In this non-linear regime, counts are lost and the number of X-rays counted no longer obeys Poisson statistics. It is important that this effect is modelled so that the number of X-rays counted can still be used to estimate the X-ray flux and the fractional error in the measured X-ray flux.

Conventionally, this effect is modelled as a dead time in the detector and the counting chain. In the dead-time model, a dead period occurs immediately following the successful detection of an X-ray. During this dead period, the detector and counting chain are blocked so that X-rays entering the detector are not counted. There are two dead-time models that are commonly used. In the non-paralysable model, the detector remains blocked for a fixed length of time, τ , following the successful detection of an X-ray. In the paralysable model, each X-ray entering the detector during the dead period extends the dead period, so that the detector remains blocked until a fixed time, τ , after the last X-ray in the dead period. The dead-time model has been studied in detail for a wide range of detection systems (for example, Faraci & Pennisi, 1983; Holford, 1982; Libert, 1977*a,b,c*, 1978; Mazoyer *et al.*, 1985; Müller, 1973, 1974; Stephan *et al.*, 1994). It is characteristic of the dead-time model that whether or not an X-ray is counted depends only on the arrival times of previous X-rays in the detector and not on the arrival times of subsequent X-rays. Thus, the dead-time model can be treated as a renewal process [see Cox (1962) for a description of renewal processes]. The dead-time model applies well when the mechanism is one in which the detector is blocked by the successful detection of an X-ray, for example, when the counting-chain electronics need a period of time in which to recover from a detection event.

In modern counting chains, the analysis and counting stages can be very fast. As examples, commercial fast SCAs that are able to resolve pulses separated by less than 10 ns and MCAs that are able to

perform conversions in less than 1 μ s are readily available. With such fast electronics, the intrinsic width of the pulses at the analysis stage is the dominant factor in determining the counting losses. The pulse width is determined both by the intrinsic width of the pulse produced by the detector and by the effect on the pulse of the amplification and shaping stage. When pulses overlap, the resulting signal at the analysis stage is the sum of the signals from each individual pulse. If we consider monoenergetic X-rays and a single-channel analyser stage, set to accept only pulses within a narrow height range about the monoenergetic height, then, if the count rate is low, every pulse will be counted. If the count rate is high, however, it becomes possible that a given pulse will overlap with the preceding or the succeeding pulse and will not be counted.

The effect of pulse overlap is illustrated in Fig. 1, which shows two pulses overlapping. The pulse shape at the analysis stage is in general not symmetrical but usually has a shorter rise and a longer decay time. In the first case in Fig. 1, the pulses are sufficiently separated such that there is no significant change in the pulse height. In the second case, the height of the second pulse is increased because of the overlap, but the peaks of both pulses still fall between the lower and upper levels of the SCA and are counted. In the third case, the peak of the second pulse is now above the upper level and is therefore not counted; only the first pulse is counted. In the fourth case, the peak of the second pulse is increased further, but the peak of the first pulse still falls between the lower and the upper levels and is counted. In the fifth case, the overlap is greater, and now the signal does not fall back below the lower level between the two pulses. The combined pulses appear as a single pulse that peaks above the upper level, and no counts are recorded by the SCA. In the sixth case, the overlap is now so great that only a single pulse is seen by the SCA, and again no counts are recorded. Clearly, depending on the time separation between two pulses, two, one or zero counts may be recorded. This result is not predicted by the dead-time model, which always allows the first pulse to be counted.

4. Pulse-overlap model of photon counting

On the basis of this analysis, we have introduced a new model to describe this process, called the pulse-overlap model. In the pulse-

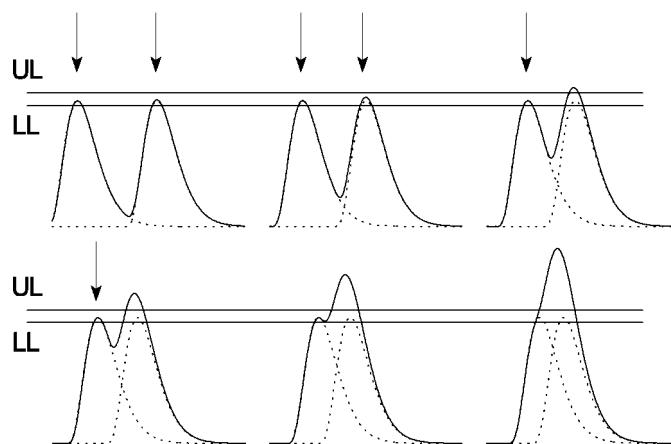


Figure 1 Reduction in the number of X-rays counted as the time difference between two successive pulses is decreased. The horizontal axis is time and the vertical axis is the signal. The signal is given by the sum of the individual pulses (shown as dotted lines). UL is the upper-level setting for the SCA and LL is the lower-level setting. The arrows indicate pulses that are successfully counted. A pulse is counted when the signal goes from below to above LL and then returns below LL again without having gone above UL.

overlap model, an X-ray is only detected if it is separated from the preceding X-ray by a time difference of more than τ_1 and from the succeeding X-ray by a time difference of more than τ_2 . Thus, the new model differs from the dead-time model in that the detection of an X-ray depends on the arrival time both of the previous and of the subsequent X-rays. The paralyzable dead-time model is a special case of the overlap model and corresponds to a τ_2 of zero and a finite τ_1 . Because the pulses are asymmetric, we allow the two characteristic times τ_1 and τ_2 to be different, and, in the example shown in Fig. 1, we expect $\tau_1 > \tau_2$. The pulse-overlap model can be used to calculate the expected number of counts in a time T when the expected number of X-rays entering the detector is λ (corresponding to an X-ray flux of λ/T). The result, derived in Appendix A [equation (15)], is

$$\bar{m} = \lambda \exp(-\lambda \tau / T), \quad (2)$$

where $\tau = \tau_1 + \tau_2$. Equation (2) is identical to the result obtained with the paralyzable dead-time model if the dead time per pulse is τ (Jenkins *et al.*, 1981). Equation (2) may also be used to estimate λ_k , the number of X-rays entering the detector in a time T , given a measurement (labelled k) in which there are m_k counts,

$$m_k = \lambda_k \exp(-\lambda_k \tau / T). \quad (3)$$

Equation (3) must be inverted to express λ_k as a function of m_k , which cannot be done analytically but is easily carried out numerically. Equation (3) is therefore used for applying a correction to data for pulse overlap. Note that at low counting rates $\lambda_k \tau / T$ is small, and the corrected number of counts becomes $\lambda_k = m_k$.

Pulse overlap affects not only the mean number of counts but also the distribution of the number of counts about the mean. In Appendix B, an expression for the standard deviation of this distribution, $s(m)$, is derived for the pulse-overlap model. $s(m)$ gives a measure of the likely deviation of the number of detected counts, m , from the mean value, \bar{m} . The result is

$$s(m) = \overline{(m - \bar{m})^2}^{1/2} = \bar{m}^{1/2} [1 + 2 \exp(-\lambda \tau' / T) - 2 \exp(-\lambda \tau / T)(1 + \lambda \tau / T)]^{1/2}, \quad (4)$$

where $\tau' = \max(\tau_1, \tau_2)$. Equation (4) can be used to estimate $s(m_k)$ from an experiment in which there are m_k counts. The purpose of the experiment is, however, to measure λ_k , the estimated number of X-rays per time T . The statistical accuracy of λ_k is given by the standard deviation of the distribution of λ_k over $k - s(\lambda_k)$, which can be calculated *via* (3) and (4). This calculation is performed in Appendix C, and the result is

$$s(\lambda_k) = \frac{\lambda_k [1 + 2 \exp(-\lambda_k \tau' / T) - 2 \exp(-\lambda_k \tau / T)(1 + \lambda_k \tau / T)]^{1/2}}{(1 - \lambda_k \tau / T) \bar{m}_k^{1/2}}. \quad (5)$$

We can define a number of counts, μ_k , such that the fractional error in λ_k is $(\mu_k)^{-1/2}$: the Poisson statistics result. To define μ_k , we set $(\mu_k)^{-1/2} = s(\lambda_k) / \lambda_k$, which gives

$$\mu_k = \frac{(1 - \lambda_k \tau / T)^2 m_k}{1 + 2 \exp(-\lambda_k \tau' / T) - 2 \exp(-\lambda_k \tau / T)(1 + \lambda_k \tau / T)}. \quad (6)$$

The estimated number of X-rays per time T is therefore λ_k [λ_k is given by (3)] and the fractional error on λ_k is $(\mu_k)^{-1/2}$ [μ_k is given by (6)]. In the absence of pulse overlap, Poisson statistics would hold and we would have $\mu_k = \lambda_k = m_k$. In the presence of pulse overlap, however, we have $\mu_k < \lambda_k$ and the statistical accuracy of the measurement is reduced. In fact, it is possible to show that $\mu_k < c_k < \lambda_k$, *i.e.* the estimated number of counts is greater than the

measured number and the number of counts used to calculate the statistical error is less than the measured number.

As an example of a detector operating at high count rates, we take a germanium solid-state detector, which could be used for a variety of measurements (for example, fluorescence EXAFS measurements or X-ray diffraction measurements), and we take a counting period T of 1 s. For 1 μ s pulse-shaping time, values of $\tau_1 = 3.0 \mu$ s and $\tau_2 = 2.0 \mu$ s are appropriate. With these values, the estimated number of X-rays (λ_k) and the number of statistical counts (μ_k) are plotted against the number of counts in the counting period (m_k) in Fig. 2. As can be seen from Fig. 2, the number of statistical counts is severely affected by pulse overlap. If there was no overlap present, the statistical counts, μ_k , would follow the Poisson line, $\mu_k = m_k$ (dotted line in Fig. 2). Even at count rates where the overlap correction required in order to estimate the number of X-rays is small, the number of statistical counts is significantly less than the number of detected counts. The number of statistical counts peaks when the number of detected counts is about 46000. The number of statistical counts at the peak is $\mu_k \sim 29000$, which corresponds to a fractional error of 0.6%. This is the limit on the statistical accuracy that can be achieved in a fixed counting time by this detector and counting chain.

5. Conclusions

We have developed the pulse-overlap model to describe the loss of counts that occurs with photon-counting detectors at high count rates. The pulse-overlap model is more general than the conventional extending dead-time model that is usually used to model counting losses. In modern synchrotron experiments with fast electronics, in which the length of the pulses is significant compared with the speed of the analysis and counting parts of the counting chain, the pulse-overlap model should be used.

We have used the pulse-overlap model to derive the correction that must be applied to the number of counts in a counting period in order to obtain an estimate for the number of X-rays in the counting period. We have also derived an expression for the statistical uncertainty (error) in this determination of the number of X-rays. The error in a measurement can be expressed in terms of an effective number of statistical counts, μ_k , for which we can apply the Poisson formula, $(\mu_k)^{-1/2}$, to calculate the fractional error. For the example of a solid-state detector with 1 μ s pulse shaping, the lowest fractional error occurs when the count rate is 46 kcounts s^{-1} , which corresponds to an effective statistical count rate of 29 kcounts s^{-1} and a fractional error of 0.6%, which is the limit on the accuracy that can be obtained with

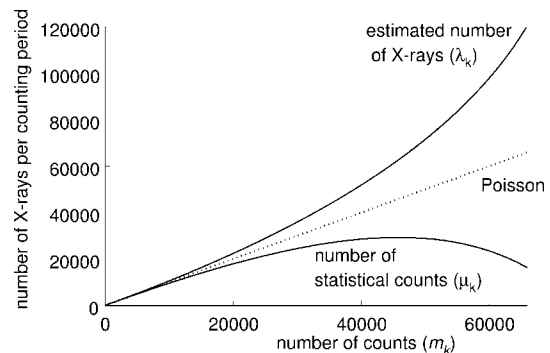


Figure 2 Overlap-corrected X-ray counts for a solid-state detector with 1 μ s pulse shaping. The top curve represents corrected X-ray counts (λ_k) and the bottom curve statistical counts (μ_k), both plotted against the number of detected counts (m_k). The dotted curve is the case when there is no pulse overlap, Poisson statistics apply and $\lambda_k = \mu_k = m_k$.

this detection system in a fixed counting period. Above this count rate, the accuracy decreases.

The error in a measurement is used to calculate error bars on the data and as the weighting for the data in model fitting routines. It is clearly important that the error is known in order that the correct error bars are published and the data are weighted correctly. We have shown that, if the normal $N^{-1/2}$ formula is applied, the error will be significantly underestimated in many applications.

APPENDIX A

Consider a counting period T , starting at time $t = 0$, in which n photons arrive in the detector at times $t_1, t_2, t_3, \dots, t_n$, where $0 \leq t_1 \leq t_2 \leq t_3 \leq \dots \leq t_n \leq T$. Consider the i th pulse, which arrives at time t_i . This pulse will only be counted if $t_i - t_{i-1} \geq \tau_1$ and $t_{i+1} - t_i \geq \tau_2$. The number of counts counted can therefore be written as

$$m(t_1, t_2, t_3, \dots, t_n) = \sum_{i=1}^{i=n} f(t_{i-1}, t_i, t_{i+1}), \quad (7)$$

where for simplicity we have defined t_0 as the time of the last pulse before time $t = 0$ and t_{n+1} as the time of the next pulse after time $t = T$. The function $f(u, v, w)$ is given by

$$f(u, v, w) = \begin{cases} 1 & \text{when } v - u \geq \tau_1 \text{ and } w - v \geq \tau_2 \\ 0 & \text{when } v - u < \tau_1 \text{ or } w - v < \tau_2. \end{cases}$$

We can write $f(u, v, w)$ in terms of the Heavyside step function $\Theta(x)$, where

$$\Theta(x) = \begin{cases} 1 & \text{for } x \geq 0 \\ 0 & \text{for } x < 0, \end{cases}$$

and therefore

$$f(u, v, w) = \Theta(v - u - \tau_1) \Theta(w - v - \tau_2).$$

The number of counts is then given by

$$m(t_1, t_2, t_3, \dots, t_n) = \sum_{i=1}^{i=n} \Theta(t_i - t_{i-1} - \tau_1) \Theta(t_{i+1} - t_i - \tau_2). \quad (8)$$

If the i th photon arrives in the detector at time t_i then the probability of the very next photon arriving in the time interval dt_{i+1} , starting at time t_{i+1} , is given by the probability that no photons arrive in the time interval t_i to t_{i+1} , which is $\exp[-\lambda(t_{i+1} - t_i)/T]$, multiplied by the probability that a photon arrives in the time interval t_{i+1} to $t_{i+1} + dt_{i+1}$, which is $(\lambda/T)dt_{i+1}$, i.e. $\exp[-\lambda(t_{i+1} - t_i)/T](\lambda/T)dt_{i+1}$. The probability of n photons arriving in the detector in time intervals $dt_1, dt_2, dt_3, \dots, dt_n$, where the intervals start at time $t_1, t_2, t_3, \dots, t_n$, is therefore given by

$$\begin{aligned} p(t_1, t_2, t_3, \dots, t_n) dt_1 dt_2 \dots dt_n &= \exp[-\lambda(t_1 - t_0)/T] (\lambda/T) dt_1 \\ &\quad \times \exp[-\lambda(t_2 - t_1)/T] (\lambda/T) dt_2 \dots \\ &\quad \times \exp[-\lambda(t_n - t_{n-1})/T] dt_n \\ &\quad \times \exp[-\lambda(t_{n+1} - t_n)/T] \\ &= \exp(-\lambda)(\lambda^n/T^n) dt_1 dt_2 \dots dt_n. \end{aligned} \quad (9)$$

The number of these n photons that are expected to be counted according to the pulse-overlap model is given by

$$\bar{m} = \sum_{n=0}^{\infty} \int_0^T dt_n \int_0^{t_n} dt_{n-1} \dots \int_0^{t_2} dt_1 p(t_1, t_2, t_3, \dots, t_n) m(t_1, t_2, t_3, \dots, t_n), \quad (10)$$

where we have set $t_0 = 0$ and $t_{n+1} = T$ and where $m(t_1, t_2, t_3, \dots, t_n)$, the number of photons counted, is given by (8). Making use of (9), the expected number of counts can be written as

$$\begin{aligned} \bar{m} &= \sum_{i=1}^{i=n} (\lambda^n/T^n) \exp(-\lambda) \int_0^T dt_n \int_0^{t_n} dt_{n-1} \dots \int_0^{t_{i+2}} dt_{i+1} \\ &\quad \times \int_0^{t_{i+1}} dt_i \Theta(t_{i+1} - t_i - \tau_1) \int_0^{t_i} dt_{i-1} \Theta(t_i - t_{i-1} - \tau_2) \\ &\quad \times \int_0^{t_{i-1}} dt_{i-2} \dots \int_0^{t_2} dt_1. \end{aligned} \quad (11)$$

The integrals can be dealt with using Laplace transforms. The convolution theorem for Laplace transforms states that for any two functions, $p(x)$ and $q(x)$, the Laplace transform of the convolution of the two functions is equal to the product of their individual Laplace transforms (see, for example, Guest, 1991),

$$\mathbf{L} \left[\int_0^T p(T-t) q(t) dt \right] = \mathbf{L}[p] \mathbf{L}[q], \quad (12)$$

where \mathbf{L} refers to the Laplace transform. The Laplace transform of (11) can easily be performed *via* the convolution theorem, (12). For example, the integral over dt_n in (11) is simplified as follows,

$$\mathbf{L} \int_0^T dt_n \int_0^{t_n} dt_{n-1} \dots = s^{-1} \mathbf{L} \int_0^T dt_{n-1} \dots,$$

where we have used $\mathbf{L}(1) = \int_0^{\infty} \exp(-xs) dx = s^{-1}$ to perform the first integral. Continuing to transform each integral in turn, we reach

$$s^{-n+i} \mathbf{L} \int_0^T dt_i \Theta(T - t_i - \tau_1) \int_0^{t_i} dt_{i-1} \Theta(t_i - t_{i-1} - \tau_2) \int_0^{t_{i-1}} dt_{i-2} \dots \int_0^{t_2} dt_1.$$

It is then necessary to apply a Laplace transform to the first Heavyside step function,

$$\begin{aligned} \mathbf{L} \Theta(x - \tau_1) &= \int_0^{\infty} \Theta(x - \tau_1) \exp(-xs) dx \\ &= \int_{\tau_1}^{\infty} \exp(-xs) dx = \exp(-\tau_1 s) s^{-1}. \end{aligned}$$

Transforming the second Heavyside step function in the same way and continuing to simplify the remaining integrals, the result is $\exp[-s(\tau_1 + \tau_2)] s^{-(n+1)}$, which may be substituted into (11) to give

$$\begin{aligned} \bar{m} &= \mathbf{L}^{-1} \sum_{n=1}^{\infty} (\lambda^n/T^n) \exp(-\lambda) \sum_{i=1}^n \exp(-s\tau) s^{-(n+1)} \\ &= \exp(-\lambda) \sum_{n=1}^{\infty} (\lambda^n/T^n) n \mathbf{L}^{-1} \exp(-s\tau) s^{-(n+1)}, \end{aligned} \quad (13)$$

where $\tau = \tau_1 + \tau_2$. The inverse Laplace transform is easily performed using standard techniques, and the summation over n can be recognized as the Taylor expansion of an exponential function. The result is

$$\bar{m} = \exp(-\lambda) \sum_{n=1}^{\infty} \lambda^n (T - \tau)^n / (T^n n!) = (1 - \tau/T) \lambda \exp(-\tau/T). \quad (14)$$

We can take advantage of the fact that $\tau \ll T$ to write the mean number of counts as

$$\bar{m} = \lambda \exp(-\lambda \tau/T). \quad (15)$$

APPENDIX B

To calculate the standard deviation of m , the number of photons counted, we make use of the following formula relating the variance

(the standard deviation squared) to the mean of m^2 ($\overline{m^2}$) and the squared mean of m (\overline{m}^2),

$$\overline{(m - \overline{m})^2} = \overline{m^2} - \overline{m}^2. \quad (16)$$

We first calculate $\overline{m^2}$ in a similar way to that in which \overline{m} was obtained in Appendix A, and write the expression as

$$\begin{aligned} \overline{m^2} &= \sum_{n=1}^{\infty} (\lambda^n / T^n) \exp(-\lambda) \sum_{i=1}^n \sum_{j=1}^n \int_0^T dt_n \int_0^{t_n} dt_{n-1} \cdots \int_0^{t_2} dt_1 \\ &\times \Theta(t_{i+1} - t_i - \tau_1) \Theta(t_i - t_{i-1} - \tau_2) \\ &\times \Theta(t_{j+1} - t_j - \tau_1) \Theta(t_j - t_{j-1} - \tau_2). \end{aligned} \quad (17)$$

This expression is more complicated than the corresponding expression in Appendix A because of the presence of the double summations (with indices i and j) and the appearance of four instead of two Heavyside step functions. To tackle this expression, we deal with the integral part of (17) first,

$$\begin{aligned} J_{i,j} &= \int_0^T dt_n \int_0^{t_n} dt_{n-1} \cdots \int_0^{t_2} dt_1 \Theta(t_{i+1} - t_i - \tau_1) \Theta(t_i - t_{i-1} - \tau_2) \\ &\times \Theta(t_{j+1} - t_j - \tau_1) \Theta(t_j - t_{j-1} - \tau_2). \end{aligned} \quad (18)$$

Four cases depending on the indices i and j can be considered separately: $j = i$, $j = i - 1$, $j = i + 1$ and $|j - i| > 1$.

For case 1, $j = i$,

$$J_{i,i} = \int_0^T dt_n \int_0^{t_n} dt_{n-1} \cdots \int_0^{t_2} dt_1 \Theta(t_{i+1} - t_i - \tau_1) \Theta(t_i - t_{i-1} - \tau_2),$$

since $\Theta(x) \Theta(x) = \Theta(x)$.

For case 2, $j = i - 1$,

$$\begin{aligned} J_{i,i-1} &= \int_0^T dt_n \int_0^{t_n} dt_{n-1} \cdots \int_0^{t_2} dt_1 \\ &\times \Theta(t_{i+1} - t_i - \tau_1) \Theta(t_i - t_{i-1} - \tau_1) \Theta(t_{i-1} - t_{i-2} - \tau_2). \end{aligned}$$

For case 3, $j = i + 1$,

$$\begin{aligned} J_{i,i+1} &= \int_0^T dt_n \int_0^{t_n} dt_{n-1} \cdots \int_0^{t_2} dt_1 \\ &\times \Theta(t_{i+2} - t_{i+1} - \tau_1) \Theta(t_{i+1} - t_i - \tau_1) \Theta(t_i - t_{i-1} - \tau_2). \end{aligned}$$

For case 4, $|j - i| > 1$,

$$\begin{aligned} J_{i,j} &= \int_0^T dt_n \int_0^{t_n} dt_{n-1} \cdots \int_0^{t_2} dt_1 \Theta(t_{i+1} - t_i - \tau_1) \Theta(t_i - t_{i-1} - \tau_2) \\ &\times \Theta(t_{j+1} - t_j - \tau_1) \Theta(t_j - t_{j-1} - \tau_2), \end{aligned}$$

where we have defined $\tau' = \max(\tau_1, \tau_2)$ and so replaced $\Theta(t - \tau_1) \Theta(t - \tau_2)$ by $\Theta(t - \tau')$. As before, we set $\tau = \tau_1 + \tau_2$. Under the summation over i and j in (18), case 1 occurs n times, cases 2 and 3 each occur $n - 1$ times, and case 4 occurs $n^2 - 3n + 2$ times. The Laplace transform is again taken, but each of the four cases are dealt with separately. The Laplace convolution theorem is used to perform the multiple integrals and, in each of the four cases, the result is independent of both i and j . The summation over i and j is therefore easily carried out by multiplying each of the four results by the number of times that each term occurs. This gives

$$\begin{aligned} \mathbf{L}(\overline{m^2}) &= \sum_{n=1}^{\infty} (\lambda^n / T^n) \exp(-\lambda) s^{-(n+1)} \{n \exp(-s\tau) \\ &+ 2(n - 1) \exp[-s(\tau + \tau')] + (n^2 - 3n + 2) \exp(-2s\tau)\}. \end{aligned} \quad (19)$$

The inverse Laplace transform of (19) gives

$$\begin{aligned} \overline{m^2} &= \sum_{n=1}^{\infty} (\lambda^n / T^n) \exp(-\lambda) (n!)^{-1} [n(T - \tau)^n \\ &+ 2(n - 1)(T - \tau - \tau')^n + (n^2 - 3n + 2)(T - 2\tau)^n]. \end{aligned} \quad (20)$$

The summation of each term in (20) is then carried out to yield

$$\begin{aligned} \overline{m^2} &= \lambda(1 - \tau/T) \exp(-\lambda\tau/T) \\ &+ 2\{\lambda[1 - (\tau + \tau')/T] - 1\} \exp[-\lambda(\tau + \tau')/T] \\ &+ [\lambda^2(1 - 2\tau/T)^2 - 2\lambda(1 - 2\tau/T) + 2] \exp(-2\lambda\tau/T). \end{aligned} \quad (21)$$

We then substitute $\overline{m^2}$, which is given in (21), and \overline{m} , which is given in (14), into (16) to get $s(m)$, the standard deviation of m : $s(m)^2 = \overline{m^2} - \overline{m}^2$. We can take advantage of the fact that $\tau_1 \ll T$, $\tau_2 \ll T$ and $\lambda \gg 1$ to remove higher-order terms and obtain the final expression for $s(m)$,

$$\begin{aligned} s(m)^2 &= \lambda \exp(-\lambda\tau/T) \\ &\times [1 + 2 \exp(-\lambda\tau'/T) - 2 \exp(-\lambda\tau/T) (1 + \lambda\tau/T)]. \end{aligned} \quad (22)$$

APPENDIX C

If for a given measurement we obtain m_k counts, we can use (14) to estimate the incident flux. Let λ_k be the estimated number of photons hitting the detector in time T , which we have calculated from m_k . It follows that m_k and λ_k are related by

$$m_k = \lambda_k \exp(-\lambda_k \tau / T). \quad (23)$$

We can also use (22) to estimate the standard deviation of m_k ,

$$s(m_k)^2 = m_k [1 + 2 \exp(-\lambda_k \tau' / T) - 2 \exp(-\lambda_k \tau / T) (1 + \lambda_k \tau / T)]. \quad (24)$$

The standard deviation, $s(\lambda_k)$, of λ_k is related to $s(m_k)$ by

$$s(\lambda_k) = s(m_k) d\lambda_k / dm_k. \quad (25)$$

The differential is calculated from (23) to yield

$$\begin{aligned} s(\lambda_k) &= \lambda_k m_k^{-1/2} [1 + 2 \exp(-\lambda_k \tau' / T) \\ &- 2 \exp(-\lambda_k \tau / T) (1 + \lambda_k \tau / T)]^{1/2} (1 - \lambda_k \tau / T)^{-1}. \end{aligned} \quad (26)$$

This result is the error on the estimated number of photons entering the detector in a time T .

References

- Cox, D. R. (1962). *Renewal Theory*. London/New York: Chapman & Hall.
- Faraci, G. & Pennisi, A. R. (1983). *Nucl. Instrum. Methods Phys. Res.* **212**, 307–310.
- Guest, P. B. (1991). *Laplace Transforms and an Introduction to Distributions*, 1st ed., *Ellis Horwood Series in Mathematics and its Applications*. Chichester: Ellis Horwood.
- Holford, R. M. (1982). *IEEE Trans. Nucl. Sci.* **29**, 629–632.
- Jenkins, R., Gould, R. W. & Gedcke, D. (1981). *Quantitative X-ray Spectrometry*, 1st ed. New York/Basel: Marcel Dekker.
- Knoll, G. F. (1989). *Radiation Detection and Measurement*, 2nd ed. New York: Wiley and Stone.
- Libert, J. (1977a). *Nucl. Instrum. Methods*, **141**, 147–151.
- Libert, J. (1977b). *Nucl. Instrum. Methods* **143**, 357–362.
- Libert, J. (1977c). *Nucl. Instrum. Methods*, **146**, 431–434.
- Libert, J. (1978). *Nucl. Instrum. Methods*, **151**, 555–561.
- Mazoyer, B. M., Roos, M. S. & Huesman, R. H. (1985). *Phys. Med. Biol.* **30**, 385–399.
- Müller, J. W. (1973). *Nucl. Instrum. Methods*, **112**, 47–57.
- Müller, J. W. (1974). *Nucl. Instrum. Methods*, **117**, 401–404.
- Stephan, T., Zehnpfennig, J. & Benninghoven, A. (1994). *J. Vac. Sci. Technol. A*, **12**, 405–410.